ELSEVIER

Journal of Power Sources 57 (1995) 125–131

JOURNAL OF POWER SOURCES

Studies on Li–Mn–O spinel system (obtained from melt-impregnation method) as a cathode for 4 V lithium batteries Part II. Optimum spinel from γ-MnOOH

Yongyao Xia, Masaki Yoshio *

Department of Applied Chemistry, Saga University, 1 Honjo, Saga 840, Japan

Received 28 July 1995; accepted 12 September 1995

Abstract

The mechanism for the formation of a spinel compound from the reaction of $LiNO_3$ with a high density γ-MnOOH is extensively investigated in terms of pore-size distribution, X-ray diffraction, thermal and chemical analyses. The reaction of MnOOH with $LiNO_3$ at about 300 °C yields a product that consists of domains of lithiated MnO_2 phase with an approximate composition of $Li_{0.3}MnO_2$. This product ultimately transforms to a disordered spinel phase of composition $LiMn_2O_{4+y}$ at 300–400 °C. The disordered spinel is converted to a well-ordered spinel as the temperature is raised above 550 °C. The oxygen content depends on the final heating temperature and atmosphere. Compounds obtained at high temperature, or in N_2, have a large capacity and unstable rechargeability. By contrast, some compounds prepared at low temperature, or with a slightly high lithium content in the starting materials, exhibit an improvement in rechargeability. The possible cause for the differences in electrochemical characteristics of both types of compound is proposed.

Keywords: Lithium; Lithium-ion batteries; Manganite; Lithiated manganese oxides; Spinel

1. Introduction

There have been many investigations of the preparation of spinel structure compounds as 4 V cathodes for lithium-ion batteries [1–3]. Significant progress has been made by the development of the melt-impregnation method. In a previous report [3], optimum spinel compounds were obtained from reaction of chemically prepared (CMD) or electrochemically prepared (EMD) manganese dioxides with $LiNO_3$ or LiOH. The main conclusion was that stoichiometric spinel compounds, $LiMn_2O_4$, can easily be prepared at a lower temperature ($T < 750$ °C) and a shorter time ($t < 48$ h) in N_2 by the melt-impregnation method. One factor affecting the electrochemical behaviour, especially the capacity, is dependent on the surface area of the resulting compounds. The latter is determined by the surface area of used MnO_2, reaction temperature and time, and the preparation technique itself. A spinel compound using CMD as a precursor exhibits larger capacity than one derived from EMD [1,3]. Furthermore, the capacity and rechargeability for these spinel electrodes is associated with the oxygen content which, in turn, depends on the preparation conditions, such as the molar ratio of Li to Mn in the starting materials, the synthesis atmosphere, the reaction temperature, and the time of reaction. This raises another issue as to how to optimize the capacity and rechargeability. The objective of the work reported here is to select high density γ-MnOOH (its density is larger than CMD and near to EMD) as a manganese source to optimize spinel-structure electrode materials, and to attempt a clarification of the above issues.

2. Experimental

All samples were prepared by the melt-impregnation method. $LiNO_3$ was used as a lithium source and was dried at 120 °C for more than 5 h to remove adsorbed water before mixing. The stoichiometric mixture of high density γ-MnOOH ($D_{bulk} = 1.538$ g/cm^3, Sedema, Belgium) and $LiNO_3$ (Li/Mn = 0.5 or 0.52 in molar ratio) was mixed thoroughly. This mixture was preheated to 260 °C for 5 h. During this period, $LiNO_3$ was melted and impregnated into the MnOOH pores, and also underwent reaction with MnOOH. Consequently, it was heated at about 410 °C to form distorted spinel, then raised to various temperatures to form well-ordered spinel in air or N_2. All samples were fast-cooled and

* Corresponding author.

SSDI 0378-7753(95)02267-7

in about 2 to 3 h, and then were directly used without any grinding.

The composition of each sample was characterized by atomic adsorption spectroscopy and chemical analysis. The manganese valence was calculated by analysis of the total manganese and oxidation powders of manganese ions according to Kozawa's method [4]. The oxygen content was evaluated from the lithium ion and manganese ion contents. The powder X-ray diffraction technique was applied to determine the crystal structure: the data were collected on a Rigaku RINT1000 X-ray diffractometer (Rigaku Ltd., Japan) with Fe Kα radiation.

A Gemini 2375 instrument was used to determine specific surface area by the BET method, and also to measure the pore-size distribution for these reacted products of MnOOH and $LiNO_3$. The samples were first heated at 200 °C for 15 min to remove adsorbed water before measurement. The formation process for spinel was investigated by thermal analysis (thermal gravimetry and differential scanning calorimetry) using a TG-8110 thermal analyser system (TAS100 system, Rigaku Ltd., Japan) at a heating rate of 10 °C/min with a 30 ml/min flow of air.

The electrochemical cell was the same as that described previously [3]. The cathode consisted of 25 mg active material and 15 mg conducting binder (acetylene black–polytetrafluoroethylene composite). The electrolyte solution was 1 M $LiPF_6$–EC/DMC (1:2 in volume). The cycling tests for the $Li/LiMn_2O_4$ system were performed on a CR2032-type button cell. The typical current rate was $C/3$ (40 mA/g), except where otherwise specified.

3. Results and discussion

3.1. Mechanism for formation of spinel compound

3.1.1. Pore-size distribution

The principle of the melt-impregnation method has been introduced earlier [3]. Here, the process of molten $LiNO_3$ impregnating the pores of MnOOH will be confirmed by the pore-size distribution measurement. The following three samples were examined: sample (a), in which MnOOH was heated at 260 °C for 2 h in air; sample (b), in which a mixture of $LiNO_3$ and MnOOH was annealed at 260 °C for 2 h in air, and sample (c), which was sample (b) washed with water. The pore-size distribution of each sample is shown in Fig. 1. It is evident that MnOOH has a number of pores with a diameter of ~50 Å. These pores are closed while the $LiNO_3$ is being melted and impregnating them; this is described by curve (b) in Fig. 1. If the impregnated $LiNO_3$ is washed with water, the pores are opened again, but the pore size shifts to a slightly larger value (curve (c), Fig. 1), and the cumulative pore volume is a little smaller than that of the original MnOOH, as shown in Table 1. This suggests that $LiNO_3$ melting is accompanied by reaction with MnOOH at 260 °C.

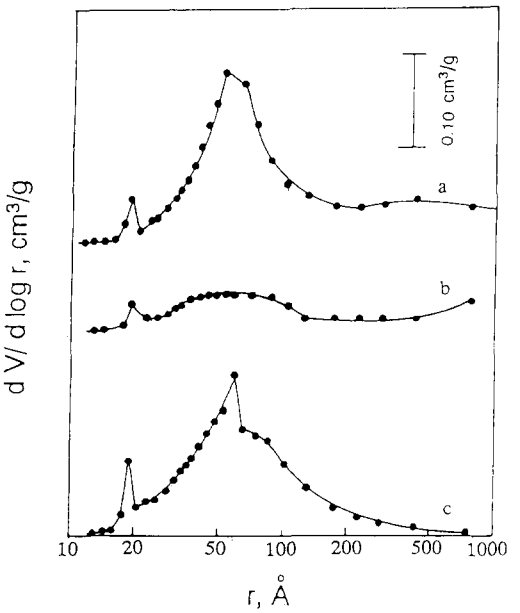

Fig. 1. Pore-size distribution of samples prepared under different conditions: (a) MnOOH heated at 260 °C for 2 h in air; (b) mixture of $LiNO_3$ and MnOOH (Li/Mn = 0.5) annealed at 260 °C for 2 h in air, and (c) sample from (b) washed with water.

Table 1
Specific surface area and cumulative pore volume of reacted products at each stage in Fig. 1 [a]

Sample	Surface area (m^2/g)	Cumulative pore volume (cm^3/g)
Sample a	25.33	0.109
Sample b	7.91	0.047
Sample c	21.23	0.081

[a] Synthesis condition for each sample is given in the caption of Fig. 1.

This will be further supported by thermal and X-ray analysis in the following section.

3.1.2. Thermal analysis

To obtain the optimum spinel, it is necessary to define the reaction mechanism. This was accomplished by a combination of thermogravimetric analysis (TG), differential scanning calorimetric analysis (DSC), X-ray diffraction spectroscopy (XRD), and chemical analysis. The DSC and TG traces for $LiNO_3$ reacting with MnOOH (Li/Mn = 0.50) in air are displayed in Fig. 2. There are four distinct peaks on the DSC curve. It is apparent that the peak at 255 °C is attributed to $LiNO_3$ melting, i.e.,

$$LiNO_3\ (\text{solid}) \longrightarrow LiNO_3\ (\text{liquid}) \qquad (\text{step 2}) \qquad (1)$$

Two shoulder peaks located at 222 °C (peak 1) and 265 °C (peak 3) are suggested to be the reaction of $LiNO_3$ and MnOOH. The XRD patterns of the mixture of $LiNO_3$ and MnOOH at 260 °C for 5 h in air is given in Fig. 3. The XRD patterns of curve (a) in Fig. 3 is characteristic of intergrown domains consisting of:

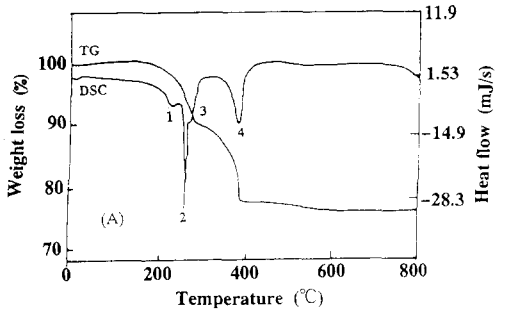

Fig. 2. Thermogravimetric and differential scanning calorimetric analyses for MnOOH in reaction with $LiNO_3$ at an annealed rate of 10 °C/min in air.

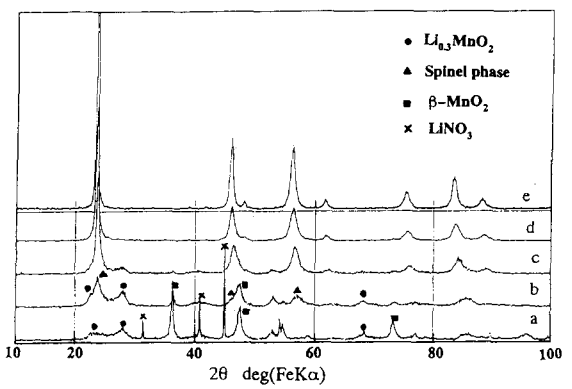

Fig. 3. Powder X-ray diffraction of reaction products of $LiNO_3$ and MnOOH (Li/Mn = 0.50) under various annealing conditions: (a) heated at 260 °C for 5 h in air; (b) heated at 300 °C for 20 h; (c) heated at 260 °C for 5 h, then further heated at 450 °C for 10 h; (d) heated at 500 °C for 10 h, and (e) heated at 260 °C for 5 h, then annealed at 410 °C for 5 h, followed by raising the temperature to 650 °C for 20 h to form well-ordered spinel.

(i) unreacted $LiNO_3$, as evident from peaks at 31.4°, 40.8° and 44.9° in 2θ;

(ii) MnO_2, as evident from peaks at 36.2°, 47.5° and 73.2° in 2θ, which results from MnOOH oxidizing to transform to β-MnO_2 (pure MnOOH occurs at 260 °C in air), and

(iii) a lithiated manganese dioxide, $Li_{0.3}MnO_2$ phase, as evident from the peaks at 23.7°, 27.8° and 68.1° in 2θ [5].

At this stage, it is thought that the peaks at 222 and 265 °C in the DSC curve should be original to $LiNO_3$ reacting with MnOOH to form lithiated Li_xMnO_2 phase, because the weight loss in the TG curve is 5.77 and 6.23% for peak 1 and peak 3, respectively. These values are much larger than 1.1%, which is the theoretical weight loss for MnOOH transformation to MnO_2. It should be noted that the formation for lithiated Li_xMnO_2 proceeds probably via two routes: one is for $LiNO_3$ reaction with MnOOH, the other one is for $LiNO_3$ reaction with MnO_2, where β-MnO_2 is transformed from MnOOH at about 260 °C. To examine this further, MnOOH was first changed to MnO_2, and then reacted with $LiNO_3$. The DSC and TG traces are given in Fig. 4. It is evident that no reaction occurs at 260 °C, while neither an endothermic/exothermic reaction peak (except for the peak of $LiNO_3$ melting) on the DSC curve nor weight loss in the TG curve

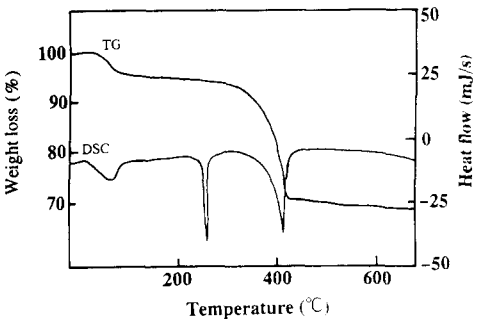

Fig. 4. Thermal analysis of MnO_2 (obtained from MnOOH at 400 °C) in reaction with $LiNO_3$ in air.

was observed. Peak 1 and peak 3 are believed to be due to the following reactions:

$$LiNO_3\ (\text{solid}) + MnOOH\ (\text{solid}) \longrightarrow$$

$$Li_{0.3}MnO_2 + HNO_3 \qquad (\text{step 1}) \quad (2)$$

$$LiNO_3\ (\text{liquid}) + MnOOH\ (\text{solid}) \longrightarrow$$

$$Li_{0.3}MnO_2 + HNO_3 \qquad (\text{step 3}) \quad (3)$$

It is highly possible that formation of lithiated $Li_{0.3}MnO_2$ with an orthorhombic unit cell system (Pnam) [6] from MnOOH, which has structure similar to orthorhombic $LiMnO_2$ (MnOOLi), passed through the route that involved lithium ion exchange.

Reaction 4 (peak 4 on DSC curve) takes place at 367 °C, which is considered to be a transformation of Li_xMnO_2 to the disordered spinel $LiMn_2O_{4+y}$ phase. The XRD pattern for the mixture of $LiNO_3$ and MnOOH heated at 450 °C for 10 h in air is characteristic of the spinel phase (curve (c), Fig. 3). The composition of this product can be represented as $LiMn_2O_{4.23}$, as confirmed by chemical analysis:

$$Li_xMnO_2 + LiNO_3 \longrightarrow$$

$$LiMn_2O_{4+y}\ (\text{disordered spinel}) \qquad (\text{step 4}) \quad (4)$$

It is noted that β-MnO_2, which is transformed from MnOOH at a temperature lower than 300 °C, also reacts with $LiNO_3$ at about 367 °C:

$$MnO_2(\beta\text{-type}) + LiNO_3 \longrightarrow$$

$$LiMn_2O_{4+y}\ (\text{disordered spinel}) \qquad (\text{step 4}) \quad (5)$$

The transformation of a disordered spinel to a well-ordered spinel begins at 500 °C, and proceeds via a loss of oxygen. A well-ordered spinel is formed at about 650 °C; the chemical formula is given in Table 2. The oxygen content in the resulting compound depends on the final heating temperature and atmosphere, which will be further detailed in the next section. Thus:

$$LiMn_2O_{4+y}\ (\text{disordered}) \longrightarrow$$

$$LiMn_2O_4\ (\text{well-ordered}) \qquad (\text{step 5}) \quad (6)$$

Table 2
Chemical analysis for products obtained from $LiNO_3$ and MnOOH under different synthesis conditions

Synthesis conditions	Composition	Mn (average valency)
260 °C, 5 h	$Li_{0.33}MnO_2$, MnO_2, $LiNO_3$	
300 °C, 20 h	$Li_{0.33}MnO_2$, $LiMn_2O_{4+y}$	3.7678
260 °C, 5 h; 450 °C	$LiMnO_{4.2326}$ ($Li_{0.5}MnO_{2.116}$)	3.7326
260 °C, 5 h; 500 °C	$LiMn_2O_{4.1432}$	3.6432
260 °C, 5 h; 410 °C, 5 h; 650 °C, 20 h	$LiMn_2O_{4.0860}$	3.5860

In summary, the net reaction of $LiNO_3$ and MnOOH is represented by:

$$LiNO_3 + 2MnOOH \longrightarrow LiMn_2O_4 + H_2O + NO_2 \quad (7)$$

3.2. Effect of heating temperature on properties of electrode material

From the above results, it is suggested that the following reaction steps are necessary to prepare the optimum spinel electrode material. The first step is to preheat the mixture at 260 °C, which will greatly improve the contact area between the lithium salt and the MnOOH and, therefore, will reduce the reaction temperature and time. The second step is further heating of the mixture at 410 °C to form the disordered spinel, which will increase the specific surface area of the resulting compound. Thus, the well-ordered spinel can be synthesized from the disordered spinel without passing through Mn_2O_3 as an intermediate product [1]. The final step is to raise the desirable temperature to form the well-ordered spinel. The effect of the final temperature on the properties of the electrode material will be investigated in detail.

3.2.1. Specific surface area

The relationship between the final heating temperature and the specific surface area are displayed in Fig. 5. The samples that correspond to each point in curve (a) were obtained from reaction of $LiNO_3$ and MnOOH preheated at 260 °C for 5 h, then further heating at 410 °C for 5 h, and final heating at various temperatures for 20 h in air. The samples in curve (b) were synthesized at 260 °C in air and at various temperatures in N_2. As expected, the surface area decreases as the temperature increases. The samples obtained in N_2 have a smaller surface area than those prepared in air. This may be due to the fact that transformation to well-ordered spinel under N_2 is easier than that under air; therefore the products are highly crystallized at the same temperature. In Fig. 5, it is of interest to note that no well-defined plateau is observed within a certain temperature range with MnOOH, in comparison with using CMD and EMD, as reported previously [1,3].

3.2.2. Crystal structure

The XRD spectra of the above compounds could be indexed to a cubic unit cell with a space group Fd3m. The calculated lattice parameter, a_0, for each of the compounds prepared in air is plotted in Fig. 6 as a function of heating

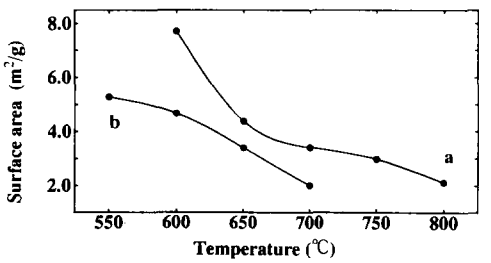

Fig. 5. Dependence of specific surface area of $LiMn_2O_4$ on synthesis temperature in: (a) air, and (b) N_2.

temperature. The a-axis expands significantly with increase in temperature, and a well-defined plateau near to 8.23 Å is detected between 650 and 750 °C. The compound prepared at 600 °C has a smaller lattice parameter a_0 of 8.22 Å. The difference in cell volume can be attributed to a difference in oxygen content, which further results in the attraction force between Mn and O. The chemical analysis for each sample is given in Table 3. The data show that the oxygen content in the spinel matrix decreases as the temperature increases.

3.2.3. Electrochemical characterization

It is easily anticipated that the difference in crystal structure also affects the charge and discharge profile of an Li/$LiMn_2O_4$ cell that contains spinel compounds from various

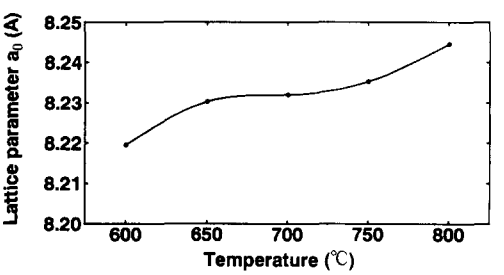

Fig. 6. Relationship between cubic lattice parameter a_0 and heat-treatment temperature.

Table 3
Chemical analysis of spinel compounds synthesized at various temperatures

Temperature (°C)	Composition	Structural formula	Mn (average valency)
600	$LiMn_2O_{4.103}$	$Li_{0.97}Mn_{1.95}O_4$	3.6044
650	$LiMn_2O_{4.086}$	$Li_{0.98}Mn_{1.96}O_4$	3.5860
700	$LiMn_2O_{4.069}$	$Li_{0.98}Mn_{1.97}O_4$	3.5690
750	$LiMn_2O_{4.014}$	$Li_{1.00}Mn_{1.99}O_4$	3.5135
800	$LiMn_2O_{4.010}$	$Li_{1.00}Mn_{2.00}O_4$	3.5102

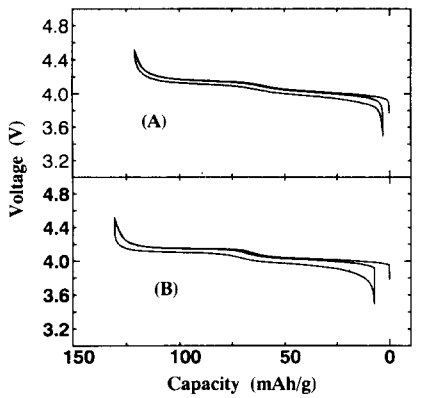

Fig. 7. Charge/discharge curves of $LiMn_2O_4$ at current rate of 0.4 mA/cm^2. Compounds were obtained from reaction of $LiNO_3$ with MnOOH at 260 °C for 5 h and 410 °C for 5 h, then at (A) 600 °C or (B) 700 °C for 20 h in air.

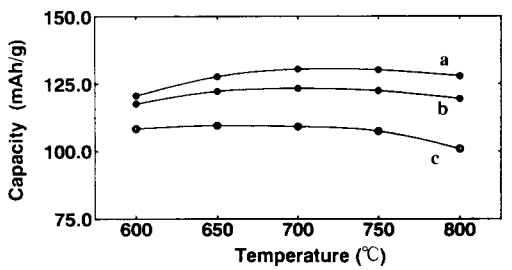

Fig. 8. Effect of synthesis temperature on battery performance of Li/$LiMn_2O_4$ cell containing various $LiMn_2O_4$ cathodes: (a) 1st charge; (b) 1st discharge, and (c) 50th discharge.

temperatures. Fig. 7 shows typical charge and discharge curves for the spinel obtained at 600 °C (sample A) and 700 °C (sample B). sample A has an initial charge capacity of 121 mAh/g with an indistinct two-step process at 4 V, whereas a stoichiometric spinel, sample B, delivers an initial charge capacity of 131 mAh/g and yields a voltage profile of a spinel electrode with a characteristic two-step process. The results of the cycling characteristics of Li/$LiMn_2O_4$ with all five compounds for the first charge and discharge, and the 50th discharge between 3.5 and 4.5 V are given in Fig. 8. The following three interesting phenomena are detected:

(i) the initial charge capacity has a tendency to increase as the heating temperature increases;

(ii) the irreversible capacity between the first charge and discharge becomes larger as the heating temperature is raised, and

(iii) the decline in capacity on cycling for samples prepared at low temperatures is more sluggish than that for samples obtained at high temperatures.

Phenomenon (i) is interrupted in terms of the Mn^{3+} content in the spinel matrix. The chemical analysis data are given in column 4 of Table 3. It is reasonable that a decrease in the Mn^{3+} content in the spinel matrix reduces the initial charge capacity, because removal of the lithium ions from the spinel framework proceeds via oxidation of Mn^{3+} to Mn^{4+}. The higher Mn^{4+} content was also considered to be a factor for improving the rechargeability, as a higher Mn^{4+} content also suppresses the following reaction [8,9]:

$$2Mn^{3+} = Mn^{4+} + Mn^{2+} \quad (8)$$

The structural formula, represented by Thackeray's expression [10], for each sample is also given in Table 3. It is evident that more Mn vacancies exist in the compounds prepared at low temperature. We propose that phenomena (ii) and (iii) are more likely to be interrupted by these 'oxygen-rich' compounds and have more stable structure for lithium-ion insertion/extraction. This will be demonstrated in Section 3.

3. Dependence of lithium content in starting material and heat-treatment atmosphere on electrochemical behaviour

The results of a slightly higher lithium content in the starting material in comparison with the stoichiometric spinel (0.50 of the molar ratio of Mn to Li) which could improve the rechargeability has already been reported for spinel compounds from CMD and EMD [3,8,11]. Fig. 9 shows the charge/discharge curves for two spinel compounds obtained

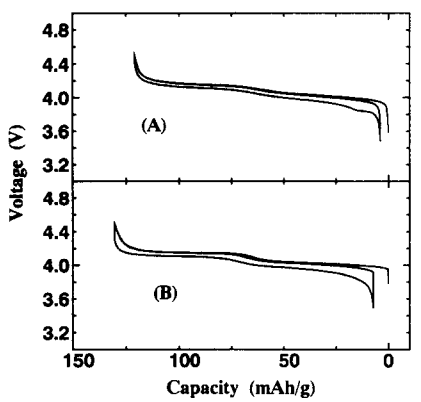

Fig. 9. Typical charge/discharge curves for spinel compounds prepared at 260 °C for 5 h, then 410 °C for 5 h, followed by heating at 700 °C in air with different lithium content in starting material. (A) Li/Mn = 0.52, and (B) 0.50.

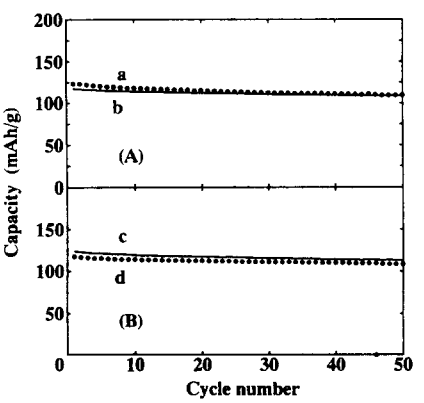

Fig. 10. Cycling behaviour of cell containing spinel compounds obtained: (A) at 700 °C in air with different Li/Mn ratios, and (B) at 600 °C with same Li/Mn molar ratio in different atmosphere. (a) Li/Mn = 0.50; (b) Li/Mn = 0.52; (c) N_2, and (d) air.

Table 4
Chemical analysis of spinel compounds obtained under different conditions

Synthesis conditions	Composition	Structural formula	Mn (average valency)
Li/Mn = 0.50, 600 °c, air	$LiMn_2O_{4.103}$	$Li_{0.97}Mn_{1.95}O_4$	3.6033
Li/Mn = 0.50, 600 °C, N_2	$LiMn_2O_{4.009}$	$Li_{1.00}Mn_{2.00}O_4$	3.5090
Li/Mn = 0.50, 700 °C, air	$LiMn_2O_{4.069}$	$Li_{0.98}Mn_{1.97}O_4$	3.5690
Li/Mn = 0.52, 700 °C, air	$Li_{1.04}Mn_2O_{4.093}$	$Li_{1.02}Mn_{1.96}O_4$	3.5732

from various lithium contents. The cycling behaviour for both compounds is presented in Fig. 10(A). The capacity fading on cycling is improved for $Li_{1.04}Mn_2O_4$ ((curve (b), Fig. 10)) at the expense of capacity; a lower initial capacity of 120 mAh/g was achieved compared with $LiMn_2O_4$, viz., 131 mAh/g. The capacity loss over the first 50 cycles is 12 and 8% of initial discharge capacity for $LiMn_2O_4$ and $Li_{1.04}Mn_2O_4$, respectively. Eventually, the difference in lithium content affects the oxygen content, as illustrated in Table 4. A change in oxygen content also influences the valence of Mn ions in the compound; therefore, it affects the total amount of the lithium ions that are removed and the rechargeability.

It is necessary to prepare the stoichiometric spinel $LiMn_2O_4$ under N_2 atmosphere, as it has been demonstrated above that a transformation of disordered spinel to well-ordered spinel is accompanied by loss of oxygen. This enables it to form a spinel compound at a lower temperature in N_2. The differences in electrochemical characteristics for both compounds obtained at the same final temperature of 600 °C under N_2 and air are shown in Fig. 11. The compound prepared under N_2 provides a larger capacity, which is in agreement with the lower oxygen content in the compound, as determined by chemical analysis (Table 4). As expected, this also results in different cycling behaviour, as described in Fig. 10(B).

In summary, the 'oxygen-rich' or 'lithium-rich' spinel compounds, $Li_{1+x}Mn_2O_{4+y}$, synthesized at a low temperature, or with a slightly higher lithium content in starting precursor, have a higher oxygen content, smaller lattice parameter a_0, lower capacity and good rechargeability. By contrast, the stoichiometric compounds, $LiMn_2O_4$, have a lower oxygen content, a larger lattice parameter (between 8.235 and 8.245 Å), and a higher capacity, but capacity fading occurs on cycling.

It is of interest to report that the difference in electrochemical behaviour for both types of compound occurs only in the higher voltage region. The shape of the charge curves in the voltage range from 3.9 to 4.4 V is shown in Fig. 12. It is evident that both compounds have the same 'S-shape' curve at a capacity of less than about 75 mAh/g; this corresponds to 0.5 molar lithium ions per unit insertion or extraction. At capacities above 75 mAh/g, the 'oxygen-rich' or 'lithium-rich' compounds still retain the 'S-shaped' curve, while the shape of the charge curve for the stoichiometric spinel compounds becomes 'L-shaped'. It is well known that the 'S-shaped' curve is characteristic of a one-phase reaction, while the 'L-shaped' curve represents a two-phase reaction. The main cause for the improved rechargeability of the 'lithium-rich', or 'oxygen-rich' spinel compounds is a homogeneous reaction over the entire intercalated region. Preliminary

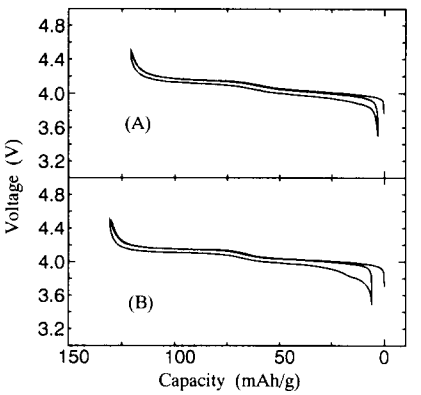

Fig. 11. Charge/discharge curves of $LiMn_2O_4$ at current rate of 0.4 mA/cm^2. Compounds obtained from reaction of $LiNO_3$with MnOOH at 260 °C for 5 h, then at 600 °C: (A) in air, (B) in N_2.

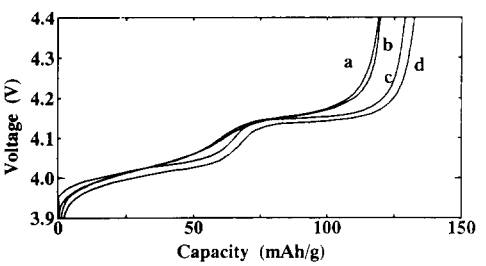

Fig. 12. Initial charge curves in voltage range 3.9 to 4.4 V for spinel electrode under different conditions: (a) Li/Mn = 0.50 at 600 °C in air; (b) Li/Mn = 0.52 at 700 °C in air; (c) Li/Mn = 0.50 at 700 °C in air, and (d) Li/Mn = 0.50 at 600 °C in N_2.

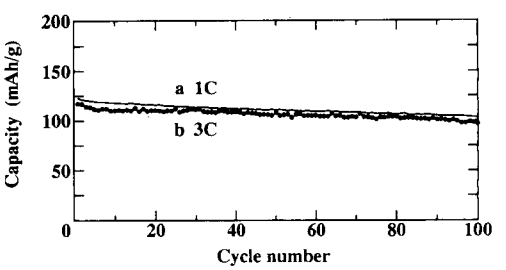

Fig. 13. Cycling behaviour of Li/$LiMn_2O_4$ cell at different current rates. $LiMn_2O_4$ obtained from $LiNO_3$ and MnOOH annealed at 260 °C for 5 h and 550 °C for 20 h in N_2. Voltage cycled between 3.5 and 4.5 V: (a) *C*; (b) 3*C*.

investigations for these compounds by XRD techniques support this suggestion [11].

In general stable rechargeability and large capacity is not common for spinel-structure electrode materials. The stable cycling capacity may be limited to 120 mAh/g for a spinel electrode. Despite this, it should be possible to optimize a igh-capacity spinel electrode with idea cycling efficiency under the principles given above. The spinel electrode is still the most promising cathode for 4 V lithium-ion batteries.

4. Cycling behaviour of optimum spinel

A stoichiometric spinel compound, synthesized at 260 °C for 5 h in air, and 550 °C for 20 h in N_2 was selected as a cathode to examine the cycling behaviour of an $Li/LiMn_2O_4$ cell at room temperature. Cells were cycled between 3.5 and 4.5 V at high current rates of 1*C* (120 mA/g) and 3*C* (360 mAh/g). The charge and discharge current was the same. The results are given in Fig. 13. The electrode materials can endure a high current rate quite satisfactorily, and can maintain 105 and 100 mAh/g at a current rate of 1*C* and 3*C*, respectively, for the first 100 cycles.

5. Conclusions

A mechanism for the formation for a spinel compound from $LiNO_3$ and γ-MnOOH is proposed. The resulting spinel passes through a route from lithiated MnO_2 (Li_xMnO_2) to a disordered spinel phase, then to a well-ordered spinel phase.

An 'oxygen-rich' or 'lithium-rich' compound is obtained at a low temperature of 600 °C, or with a slightly higher lithium content (Li/Mn = 0.52) in air by the melt-impregnation method. These compounds exhibit improved rechargeability, but deliver a slightly lower capacity of 120 mAh/g. The optimum conditions for the preparation of stoichiometric spinel are under a N_2 atmosphere at low temperatures (550 °C), or in air at a higher temperatures.

The difference in the electrochemical behaviour for both types of compound results from the different oxygen content in the spinel matrix. The latter affects the crystal structure. The main difference in the battery profile occurs in the high voltage region. The shape of charge curve for the 'oxygen-rich' or 'lithium-rich' compound is 'S-shaped' in the range of $0 < x < 0.5$ in $Li_xMn_2O_4$. This indicates a homogeneous reaction, whereas the stoichiometric $LiMn_2O_4$ compound displays an 'L-shaped' curve. This corresponds to a two-phase reaction.

Acknowledgements

The authors would like to thank Sedema Ltd., Belgium, for the supply of high density MnOOH and Dr J.C. Rousche for his helpful discussion. They are grateful to the grants-in-aid for Scientific Research from the Japanese Ministry of Education (Nos. 06453124 and 06555188) for partial support of this research.

References

[1] V. Manev, A. Momchilov, A. Nassalevska and A. Kozawa, *J. Power Sources, 43/44* (1993) 551.
[2] J.M. Tarascon, E. Wang, F.K. Skokoohi, W.R. McKinnon and S. Colson, *J. Electrochem. Soc., 138* (1991) 2860.
[3] Y. Xia, H. Takeshige, H. Noguchi and M. Yoshio, *J. Power Sources, 56* (1995) 61.
[4] A. Kozawa, *Memo. Fac. Nagoya, Uni., 11* (1959) 243.
[5] M. Yoshio, S. Inoue, M. Hyakutake, G. Piao and H. Nakamura, *J. Power Sources, 34* (1991) 147.
[6] M.M. Thackeray, M.H. Rossouw, R.J. Gummow, D.C. Liles, K. Pearce, A. De Kock, W.I.F. David and S. Hull, *Electrochim. Acta, 38* (1993) 1259.
[7] A.F. Wells, *Structural Inorganic Chemistry*, Clarendon Press, Oxford, 4th edn., 1975.
[8] R.J. Gummow, A. De Kock and M.M. Thackeray, *Solid State Ionics, 69* (1994) 59.
[9] J.M. Tarascon, W.R. McKinnon, F. Coowar, T.N. Bowmer, G. Amatucci and D. Guyomard, *J. Electrochem. Soc., 141* (1994) 1421.
[10] A. de Kock, M.H. Rossouw, L.A. de Picciotto and M.M. Thackeray, *Mater. Res. Bull., 25* (1990) 657.
[11] M. Yoshio, H. Noguchi, T. Miyashita, H. Nakamura and A. Kozawa, *J. Power Sources, 54* (1995) 483.